Single element ultrasonic imaging of limb geometry: an in-vivo study with comparison to MRI

Single element ultrasonic imaging of limb geometry: an in-vivo study with comparison to MRI

Xiang Zhang, Jonathan R. Fincke, Brian W. Anthony

Xiang Zhang, Jonathan R. Fincke, Brian W. Anthony, "Single element ultrasonic imaging of limb geometry: an in-vivo study with comparison to MRI," Proc. SPIE 9790, Medical Imaging 2016: Ultrasonic Imaging and Tomography, 97901R (1 April 2016); doi: 10.1117/12.2216542

SPIE.

Event: SPIE Medical Imaging, 2016, San Diego, California, United States

Single Element Ultrasonic Imaging of Limb Geometry: An In-Vivo Study With Comparison to MRI

Xiang Zhang, Jonathan R. Fincke, and Brian W. Anthony

Massachusetts Institute of Technology,
77 Massachusetts Ave,
Cambridge, MA 02141, USA

ABSTRACT

Despite advancements in medical imaging, current prosthetic fitting methods remain subjective, operator dependent, and non-repeatable. The standard plaster casting method relies on prosthetist experience and tactile feel of the limb to design the prosthetic socket. Often times, many fitting iterations are required to achieve an acceptable fit. Use of improper socket fittings can lead to painful pathologies including neuromas, inflammation, soft tissue calcification, and pressure sores, often forcing the wearer to into a wheelchair and reducing mobility and quality of life. Computer software along with MRI/CT imaging has already been explored to aid the socket design process. In this paper, we explore the use of ultrasound instead of MRI/CT to accurately obtain the underlying limb geometry to assist the prosthetic socket design process. Using a single element ultrasound system, multiple subjects' proximal limbs were imaged using 1, 2.25, and 5 MHz single element transducers. Each ultrasound transducer was calibrated to ensure acoustic exposure within the limits defined by the FDA. To validate image quality, each patient was also imaged in an MRI. Fiducial markers visible in both MRI and ultrasound were used to compare the same limb cross-sectional image for each patient. After applying a migration algorithm, B-mode ultrasound cross-sections showed sufficiently high image resolution to characterize the skin and bone boundaries along with the underlying tissue structures.

Keywords: limb imaging, prosthetic fitting, ultrasound, single element ultrasound, MRI

1. INTRODUCTION

Current prosthetic socket design and fabrication methods remain largely artisanal. The proper prosthetic fit replies on proper mechanical coupling between the residual limb and the prosthetic socket. Ideal design and coupling at the limb to socket interface encourages muscle usage, relieves pressure at sensitive areas, and distributes stresses to more load tolerant regions. For lower limb amputees, the prosthetic interface transfers static and dynamic loads from the socket through the soft tissue to the bone during gait. To design the proper socket fitting, biomechanical understanding of the underlying soft tissue structure, tissue stiffness, and bone geometry is essential.[1] However, the current socket fitting procedure relies on plaster casting of the residual limb with palpation of the limb surface by the prosthetist to estimate the regional tissue stiffness. The process is mostly subjective and operator dependent; multiple fittings are often required to achieve the desired fit. Though effective in some instances, this fitting method is time consuming, expensive, and qualitative. Quantitative measurements of the residual limb using modern imaging methods such as computed tomography (CT), magnetic resonance imaging (MRI), and ultrasound can improve the prosthetic fitting procedure by informing the designer on the internal limb geometry and the underlying tissue structure. Computer-aided design/manufacturing (CAD/CAM) has already been explored as an addition to the prosthetic design process.[2] Incorporation of medical imaging techniques into the CAD/CAM process has the potential to improve the design accuracy and functionality. Of the three imaging methods, ultrasound has the distinct advantage of being low-cost, portable, and non-ionizing, though typically lower in image resolution. However, recent developments in ultrasound tomography in soft tissue have shown high-resolution images comparable to those of MRI.[3] Motivated by results in soft tissue, we designed

Corresponding author: X. Zhang: E-mail: xzhang88@mit.edu,
J. Fincke: E-mail: jfincke@mit.edu,
B. Anthony: E-mail: banthony@mit.edu

Medical Imaging 2016: Ultrasonic Imaging and Tomography, edited by Neb Duric, Brecht Heyde, Proc. of SPIE
Vol. 9790, 97901R · © 2016 SPIE · CCC code: 1605-7422/16/$18 · doi: 10.1117/12.2216542

and built a single element tomographic system to leverage the ultrasound tomography (UST) technique for limb imaging.[4] To apply UST imaging for limbs, new algorithms and hardware accommodating complex scattering and attenuation of ultrasound in bone need to be explored. The developed single element system enables the necessary flexibility to test varying algorithms, sampling strategies, and transducers. In this paper, we explore the feasibility of using B-mode ultrasound to capture the necessary limb geometry for improving prosthetic fittings. Patient limbs were scanned in both MRI and ultrasound to compare the imaged limb geometries.

2. METHODS

2.1 Scanning System

A single element UST system was designed and built previously for UST algorithm development for limb scanning. Two submerged single element transducers move independently, radially and vertically, in a water tank around the scan target. Full cylindrical backscatter and tomographic scanning is possible on the system. The system has been calibrated and is within specifications for single element ultrasound imaging up to 5 MHz.[4] For B-mode imaging and comparison to MRI, one transducer was removed and a single transducer was used for imaging. The mechanical positioning and data acquisition systems are is shown in Fig. 1.

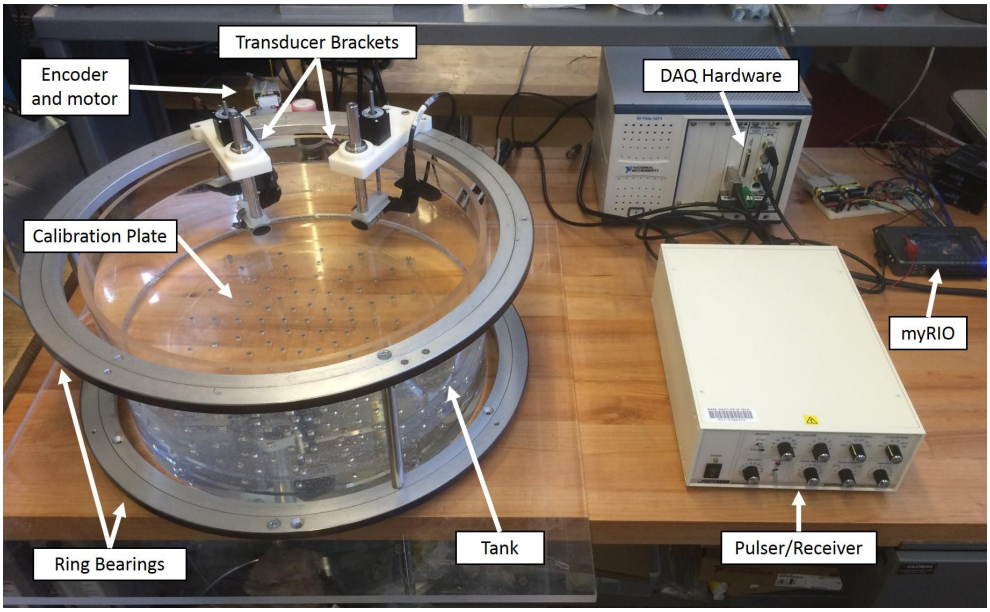

Figure 1: Full single element scanning system with both transmit and receive transducer bracketing attached.

2.2 Transducers and FDA Calibration

To cover a sufficiently large region of interest (ROI) at the tank center, custom cylindrically focused transducers were selected. Eventual implementation of UST techniques will require through bone ultrasound transmission, necessitating the need for lower frequency transducers.[5] To test the effects of reducing transducer frequencies on human subjects, all were imaged with 1, 2.25, and 5 MHz center frequency transducers for comparison. In compliance with the Massachusetts Institute of Technology institute review board, all transducers were calibrated following the FDA and NEMA acoustic output standards prior to human scanning.[6,7] The derated spatial peak-pulse temporal-average intensities, I_{spta3}, and the derated spatial peak-pulse spatial-average intensities, I_{sppa3} for each transducer were confirmed to be within the outlined FDA exposure limits, shown in Table 1.

Table 1: Measured acoustic exposure for all transducers compared to the limits set forth by the FDA for peripheral vessel imaging.[6] At maximum operating levels, the measured I_{spta3} for all transducers are at least 7 orders of magnitude below the FDA limits and the corresponding I_{sppa3} exposures are 1 order of magnitude below the threshold.

Frequency	I_{spta3}	I_{sppa3}
1 MHz	$2.9 \times 10^{-}6$ mW/cm^2	3 W/cm^2
2.25 MHz	$6.9 \times 10^{-}6$ mW/cm^2	7 W/cm^2
5 MHz	$1.2 \times 10^{-}5$ mW/cm^2	12 W/cm^2
FDA Limits	720 mW/cm^2	120 W/cm^2

2.3 MRI Imaging and Alignment

For comparison of image quality, subjects limbs were scanned on a MRI scanner at the McGovern Institute. Transverse slices of each subject's lower forearms were taken. For visualization of the bone and muscle boundaries, two-echo ultra-short echo-time (UTE) sequences were used.[8] For the available MRI system, 1 mm isotropic voxel resolution was achieved. DICOM data post-processed to select proper slices for comparison. Fiducials (Beekley Medical) visible in both MRI and ultrasound were placed on each subject for slice alignment.

2.4 Image Reconstruction

Image distortion due to the wide transducer beamwidth was corrected using a migration algorithm.[4] In cylindrical scanning, each received echo is actually a summation of all echoing objects at the same radii from the transducer. This creates a sinusoidal diffraction pattern for each point source within the ROI. However, because the expected diffraction pattern for any point source within the ROI can be calculated theoretically, the diffraction pattern from every point source can be collapsed and migrated back to their original form and position.[9]

3. RESULTS

Five MRI and B-mode scans were completed on three subjects. All subjects consented and were imaged following MIT's institute review board approval guidelines. MRI imaging of each subject's lower forearm was completed prior to B-mode imaging. Data from one subject's forearm has been omitted due to large motion artifacts during the MRI scan. Transverse image slices of each subject's forearms are presented in Section 3.1 and 3.2.

3.1 B-mode Transverse Sections

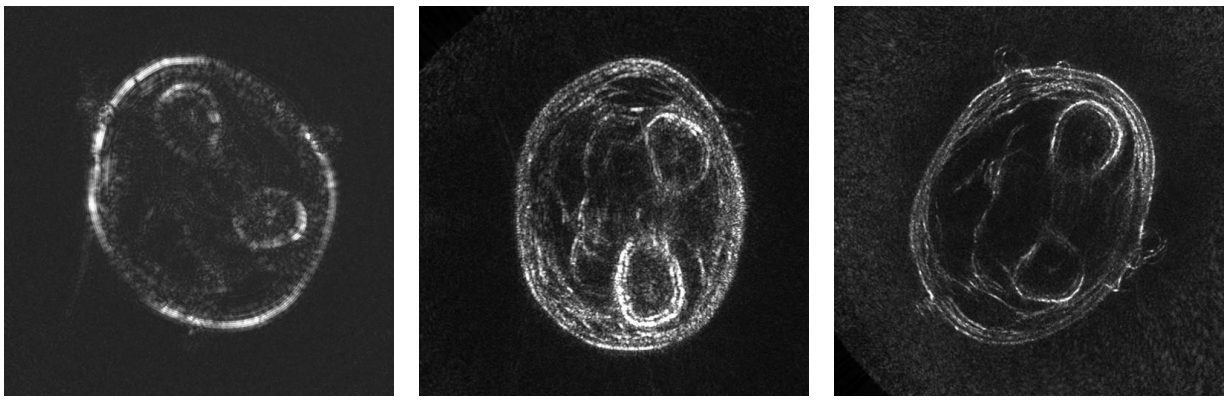

(a) 1 MHz (b) 2.25 MHz (c) 5 MHz

Figure 2: Subject 1: Left forearm.

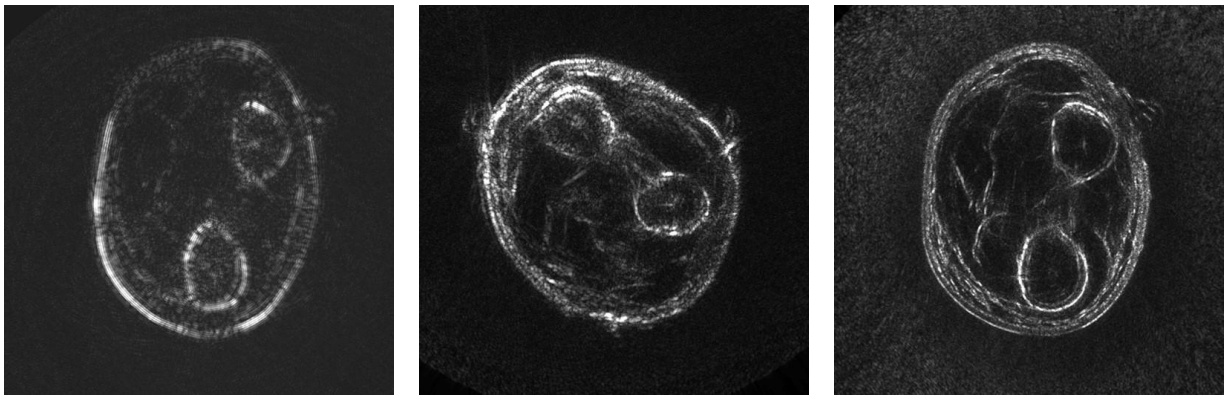

(a) 1 MHz (b) 2.25 MHz (c) 5 MHz

Figure 3: Subject 1: Right forearm.

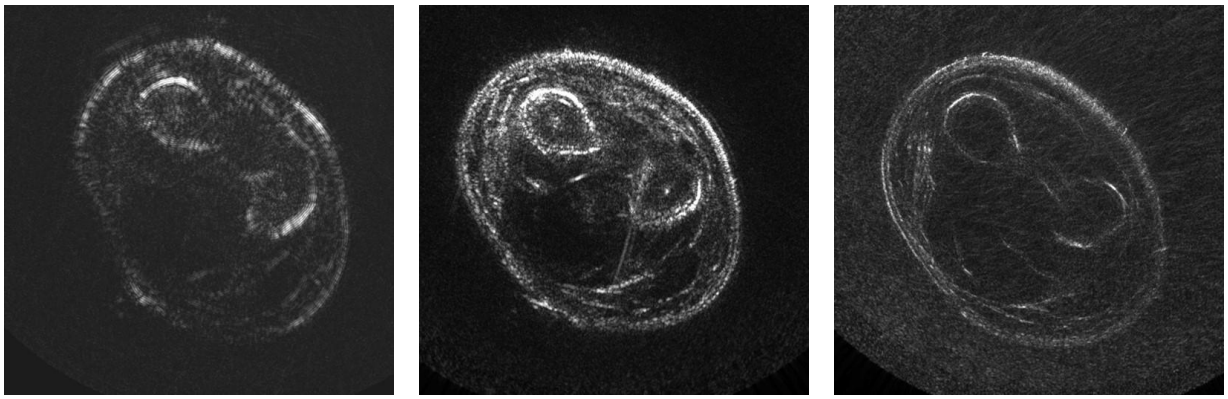

(a) 1 MHz (b) 2.25 MHz (c) 5 MHz

Figure 4: Subject 2: Left forearm.

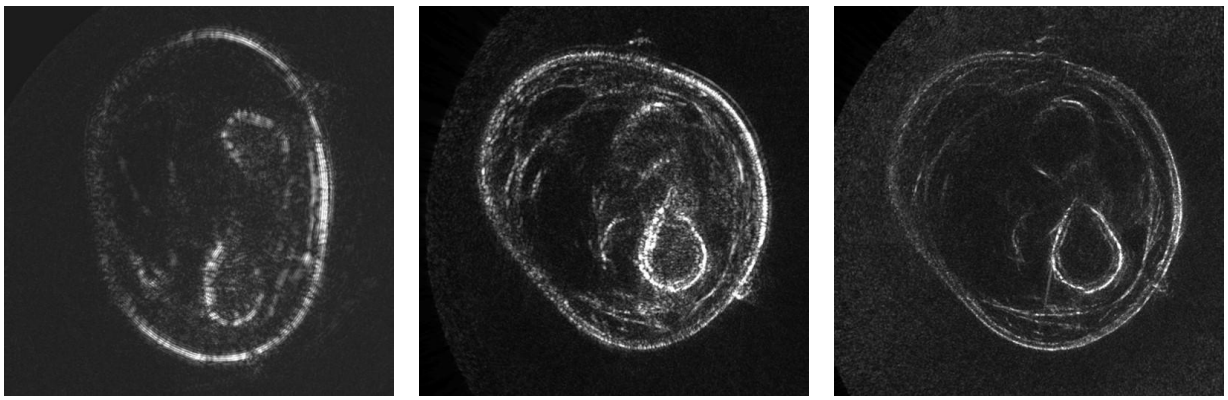

(a) 1 MHz (b) 2.25 MHz (c) 5 MHz

Figure 5: Subject 2: Right forearm.

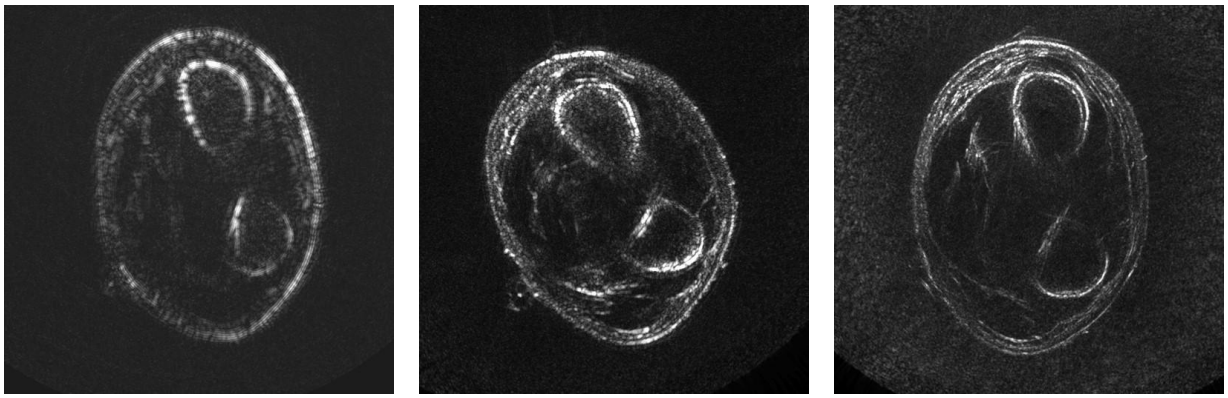

(a) 1 MHz (b) 2.25 MHz (c) 5 MHz

Figure 6: Subject 3: Left forearm.

3.2 MRI Transverse Sections

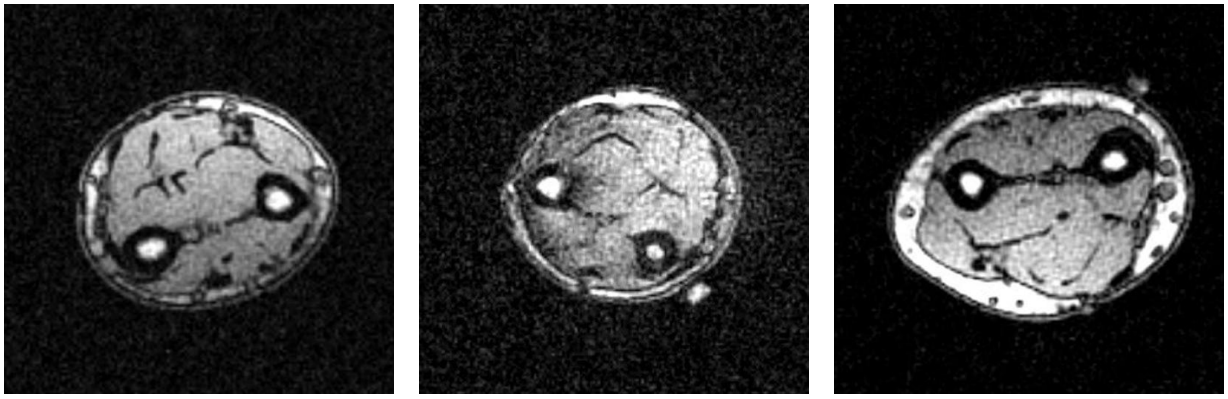

(a) Subject 1: Left forearm MRI (b) Subject 1: Right forearm MRI (c) Subject 2: Left forearm MRI

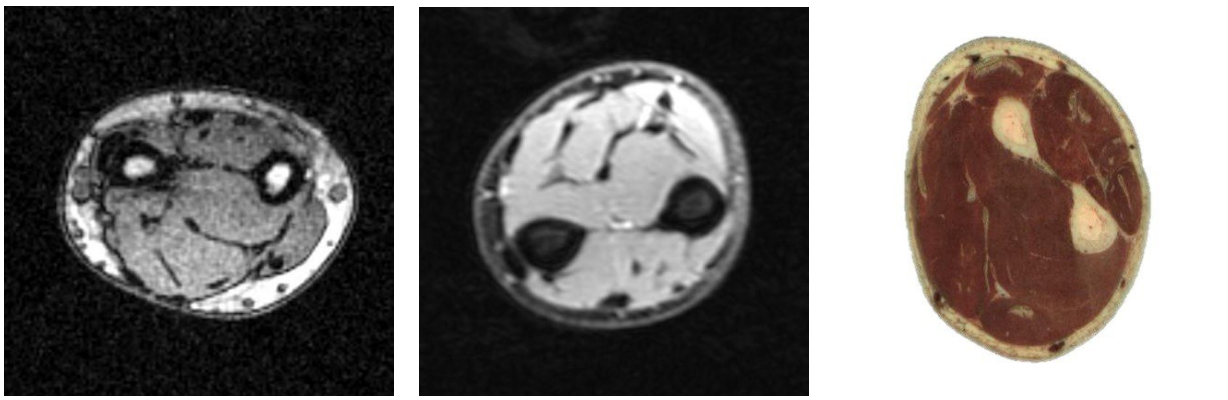

(d) Subject 2: Right forearm MRI (e) Subject 3: Left forearm MRI (f) Visible Human forearm slice[10]

Figure 7: All subject MRI's using the 2-echo UTE scan sequence and a representative transverse forearm slice from the Visible Human Project.[10]

4. DISCUSSION

For each subject, at all frequencies (1, 2.25, 5 MHz), the skin/water and and muscle/bone boundaries can be seen. The fat/muscle boundaries can be seen at the higher frequencies, particularly in Fig. 2c, 3c, and 6c. For lower frequencies, the clarity of the fat/muscle boundaries degrades, as well as the fidelity of the exact bone boundary. This is degradation outlines the trade-off between reducing frequencies for through bone transmission and the corresponding reduction in image resolution. Based on clinical needs for prosthetic fitting and manufacturing, it may be necessary to differentiate frequencies for back-scatter imaging versus transmission imaging.

Comparing transverse B-mode to MRI cross sections, the dominate features; bone, skin, and fat boundaries; are present in both modalities. MRI images in Fig, 7 show better segmentation between the muscle bundles, additional features within the fat layers, and the marrow boundaries within the bone. For prosthetic fitting, marrow boundaries within the radius/ulna and features within the muscle/fat are less critical compared to the bone and skin boundaries. Load bearing in the residual limb during gait is combined loading of all tissues layers; effective coupling design of the socket/limb interface should distribute stresses within the limb, requiring knowledge of the stiffness distribution within the limb.[1] Characterization of high stiffness regions with ultrasound will require implementation of UST and sound speed mapping.[11,12] B-mode imaging should provide accurate representation of bone and skin boundaries while transmission imaging should provide spatial stiffness. B-mode images presented in Section 3.1 have the highest contrast at the bone and skin boundaries; segmentation of these boundaries and incorporation of the spatial stiffness into CAD/CAM software will feed into future quantitative prosthetic socket designs.

5. CONCLUSION AND FUTURE WORK

In this study, we have demonstrated the feasibility of using a low-cost single element ultrasound system to capture limb geometries at a sufficient resolution to guide prosthetic socket design. We have expanded upon the data set collected previously on the system and demonstrated that the capability of collecting *in-vivo* data.[4] Leveraging the flexibility of the designed system, multiple frequency transducers have been tested on three separate subjects with a total of five image targets. Comparisons of B-mode versus MRI scans of each target are presented and show congruence between the two imaging modalities for the each limb. B-mode images show sufficient resolution to segment the bone and skin boundaries.

Clinical use of medical imaging for improving prosthetic fittings will require robust segmentation of bone, fat and muscle boundaries as well as quantitative analysis of tissue properties within the residual limb. In addition, implementation of CAD/CAM software for streamlined manufacturing of custom prosthetics will require generation of solid models for each imaged limb.[2] Qualitative comparison of MRI and B-mode images presented in this paper show promise that B-mode ultrasound can extract the necessary limb geometries. However, tissue stiffness as a function of the spatial limb geometry is also necessary for effective prosthetic socket design.[13] Implementation of UST techniques used in soft tissue could provide a solution. Through transmission of ultrasound in *in-vivo* targets with bone presents an interesting set of new challenges; characterization of complex wave propagation through bone will necessitate innovations in both hardware and algorithms.[5] The presented flexible single element system will support future development and validation of new algorithms.[4]

Future work on the system will include: B-mode/UST imaging of additional phantom and *in-vivo* targets, volumetric reconstruction of scanned geometries, robust segmentation of layers and volumes, and integration of ultrasound imaging into the prosthetic design work-flow. Results and insights gained from the projected work will inform and guide future clinical system designs.

ACKNOWLEDGMENTS

The authors would like to thank Steven Shannon at the McGovern Institute for Brain Research at MIT for his MRI and imaging expertise and Bryan Ranger of the Device Realization Laboratory at MIT for his help and guidance. This work was supported by the Skolkovo Institute of Science and Technology.

REFERENCES

[1] Mak, A. F., Zhang, M., and Boone, D. A., "State-of-the-art research in lower-limb prosthetic biomechanics-socket interface: a review.," *Journal of rehabilitation research and development* **38**, 161–74 (jan 2001).

[2] Topper, A. K. and Fernie, G. R., "Computer-aided design and computer-aided manufacturing (CAD/CAM) in prosthetics.," *Clinical orthopaedics and related research* , 39–43 (jul 1990).

[3] Ranger, B., Littrup, P., Duric, N., Li, C., Schmidt, S., Lupinacci, J., Myc, L., Szczepanski, A., Rama, O., and Bey-Knight, L., "Breast imaging with ultrasound tomography: a comparative study with MRI," *Proceedings of SPIE* **7629**, 762906–1–762906–9 (2010).

[4] Zhang, X., Fincke, J., Kuzmin, A., Lempitsky, V., and Anthony, B., "A single element 3D ultrasound tomography system," in [*Proceedings of the Annual International Conference of the IEEE Engineering in Medicine and Biology Society, EMBS*], **2015-Novem**, 5541–5544 (aug 2015).

[5] Laugier, P. and Haiat, G., "Bone quantitative ultrasound," *Bone Quantitative Ultrasound* , 1–468 (2011).

[6] U.S. Department of Health and Human Services, "Information for Manufacturers Seeking Marketing Clearance of Diagnostic Ultrasound Systems and Transducers," 1–64 (2008).

[7] National Electrical Manufacturers Association, "Acoustic Output Measurement Standard for Diagnostic Ultrasound Equipment, Revision 3," (2009).

[8] Robson, M. D., Gatehouse, P. D., Bydder, M., and Bydder, G. M., "Magnetic resonance: an introduction to ultrashort TE (UTE) imaging.," *Journal of computer assisted tomography* **27**, jan.

[9] Norton, S. J., "Reconstruction of a two-dimensional reflecting medium over a circular domain: Exact solution," *The Journal of the Acoustical Society of America* **67**(4), 1266 (1980).

[10] Ackerman, M., "The Visible Human Project," *Proceedings of the IEEE* **86**, 504–511 (mar 1998).

[11] Duric, N., Littrup, P., Poulo, L., Babkin, A., Pevzner, R., Holsapple, E., Rama, O., and Glide, C., "Detection of breast cancer with ultrasound tomography: first results with the Computed Ultrasound Risk Evaluation (CURE) prototype.," *Medical physics* **34**(2), 773–785 (2007).

[12] Li, C., Duric, N., Littrup, P., and Huang, L., "In vivo Breast Sound-Speed Imaging with Ultrasound Tomography," *Ultrasound in Medicine and Biology* **35**(10), 1615–1628 (2009).

[13] Douglas, T., Solomonidis, S., Sandham, W., and Spence, W., "Ultrasound imaging in lower limb prosthetics," *IEEE Transactions on Neural Systems and Rehabilitation Engineering* **10**(1), 11–21 (2002).